Journal of Medicinal Chemistry

Article

pubs.acs.org/jmc

Nanomolar Potency and Metabolically Stable Inhibitors of Kidney Urea Transporter UT-B

Marc O. Anderson,*[,†] Jicheng Zhang,[†] Yan Liu,[†] Chenjuan Yao,[‡] Puay-Wah Phuan,[‡] and A. S. Verkman[‡]

[†]Department of Chemistry and Biochemistry, San Francisco State University, San Francisco, California 94132-4136, United States

[‡]Department of Medicine and Physiology, University of California, San Francisco, California 94143-0521, United States

Supporting Information

ABSTRACT: Urea transporters, which include UT-B in kidney microvessels, are potential targets for development of drugs with a novel diuretic ('urearetic') mechanism. We recently identified, by high-throughput screening, a triazolothienopyrimidine UT-B inhibitor, **1**, that selectively and reversibly inhibited urea transport with IC_{50} = 25.1 nM and reduced urinary concentration in mice (Yao et al. *J. Am. Soc. Nephrol.*, in press). Here, we analyzed 273 commercially available analogues of **1** to establish a structure–activity series and synthesized a targeted library of 11 analogues to identify potent, metabolically stable UT-B inhibitors. The best compound, {3-[4-(1,1-difluoroethyl)benzenesulfonyl]thieno[2,3-*e*][1,2,3]triazolo[1,5-*a*]pyrimidin-5-yl}thiophen-2-ylmethylamine, **3k**, had IC_{50} of 23 and 15 nM for inhibition of urea transport by mouse and human UT-B, respectively, and ~40-fold improved in vitro metabolic stability compared to **1**. In mice, **3k** accumulated in kidney and urine and reduced maximum urinary concentration. Triazolothienopyrimidines may be useful for therapy of diuretic-refractory edema in heart and liver failure.

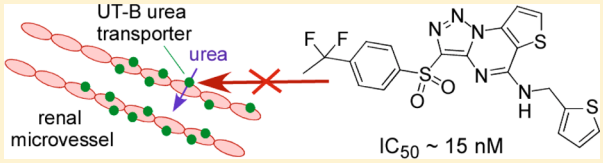

INTRODUCTION

Urea transport across kidney tubular epithelial cells and microvascular endothelia is required for generation of a concentrated urine by countercurrent multiplication and exchange mechanisms.[1,2] Kidney tubules express urea transporter A (UT-A) isoforms, encoded by the *SLc14A2* gene, and kidney microvessels express UT-B, encoded by the *SLc14A1* gene.[3−5] Knockout mice lacking UT-B[6,7] or various UT-A isoforms[8−11] have reduced urinary concentrating ability, providing a rationale for the development of UT inhibitors as "urearetics" with a novel diuretic mechanism of action. Conventional diuretics that target salt transporters can be of limited efficacy in some fluid-retaining states such as advanced congestive heart failure and cirrhosis.

Until recently, available UT inhibitors included urea analogues, which have millimolar IC_{50}, and the nonselective membrane intercalating agent phloretin.[12] Utilizing an erythrocyte lysis-based high-throughput screen, we identified phenylsulfoxyoxozole inhibitors of human UT-B with $IC_{50} \approx$ 100 nM.[13] However, the phenylsulfoxyoxozoles poorly inhibited rodent UT-B, precluding their testing in rodents. Recently, a screen of 100 000 synthetic small molecules yielded triazolothienopyrimidine UT-B inhibitors.[14] The most potent compound **1** reversibly inhibited mouse UT-B urea transport with IC_{50} = 25.1 nM by a competitive mechanism and was highly selective for UT-B over UT-A isoforms. Though **1** is nontoxic, its metabolic stability was poor, requiring administration of large quantities in mice to obtain therapeutic levels in kidney and reduce urinary concentration.

Here, we established structure–activity relationships (SARs) of triazolothienopyrimidine UT-B inhibitors, with the goal of identifying analogues of **1** with high potency and improved metabolic stability. Our strategy was to deduce initial SAR from functional testing of commercially available triazolothienopyrimidines, determine the site(s) of metabolism of **1**, and synthesize a library of targeted analogues. One compound with excellent UT-B inhibition potency and in vitro metabolic stability was further characterized and tested in mice.

RESULTS AND DISCUSSION

Structure–Activity Relationships of Triazolothienopyrimidine UT-B Inhibitors. Initial SAR was deduced from analysis of 273 commercially available triazolothienopyrimidine analogues of **1**. UT-B inhibition was measured by an erythrocyte lysis assay. Of the compounds tested, 103 compounds inhibited UT-B urea permeability by >60% at 25 μM. Twelve compounds had IC_{50} < 500 nM, with compound **1** having the lowest IC_{50}. Figure 1A shows concentration–inhibition data for selected inhibitors. The data fitted well to a single-site inhibition model with near 100% inhibition at high concentration. Table S1 (Supporting Information) provides IC_{50} for the 75 compounds (**2aa**–**2cv**) with greatest inhibition potency, and metabolic stability data for a selected subset.

SAR analysis indicated greatest potency for thiophene-2-methylamine at R^2. Replacing the heteroaryl sulfur atom by oxygen (thiophene → furan) increased IC_{50} substantially (compare **1** and **2bo**, Table S1). Bulky R^2 groups containing cyclic rings such as morpholine (**2bp**, IC_{50} = 5.6 μM) and piperidine (IC_{50} > 25 μM, not shown) greatly reduced activity. The reduced activity with inclusion of a bulky group is consistent with our previous computational docking of **1** to a

Received: April 7, 2012
Published: June 13, 2012

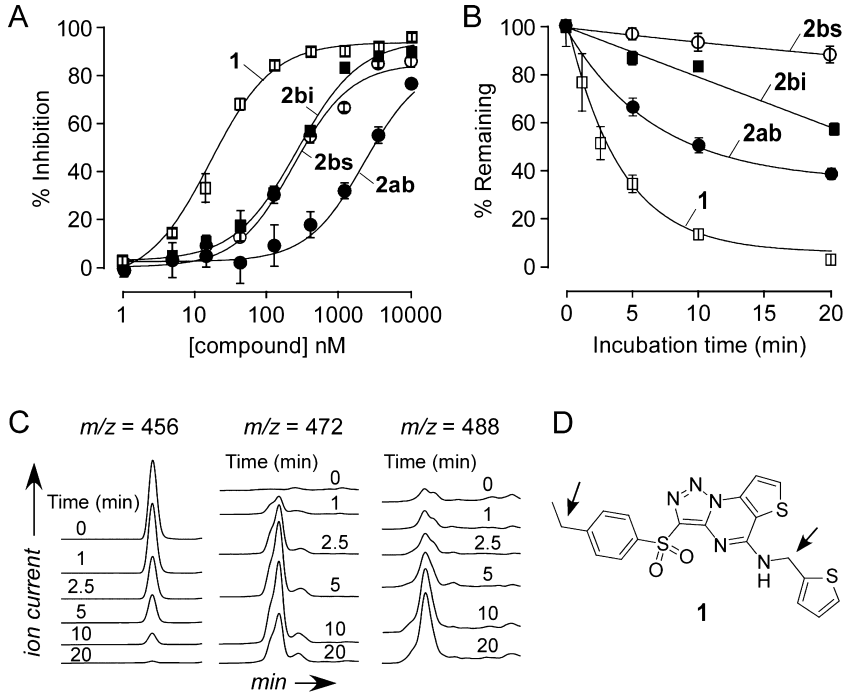

Figure 1. UT-B inhibition potency and metabolic stability of selected triazolothienopyrimidine analogues. See Table S1 (Supporting Information) for summary of potency and metabolic stability data for all compounds: (A) concentration−inhibition data from erythrocyte lysis assay for indicated compounds (SE, $n = 3$); (B) in vitro metabolic stability data shown as kinetics of disappearance of indicated parent compounds following incubation with hepatic microsomes and NADPH; (C) LC/MS traces showing disappearance of **1** and appearance of metabolites at $m/z = 472$ and 488; (D) structure of **1** showing putative sites of metabolism.

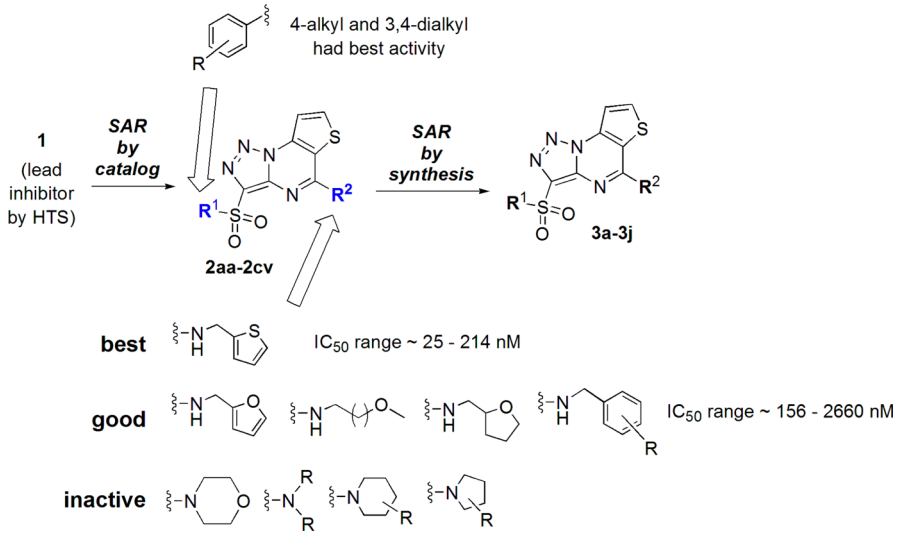

Figure 2. General strategy for optimization of triazolothienopyrimidines. Shown are structural determinants of triazolothienopyrimidine inhibition activity identified from commercially available analogues ("SAR-by-catalog") followed by synthesized of a focused library.

homology model of UT-B showing a sterically tight fit near the amidine linkage.[14] Analogues containing a flexible chain with a terminal ether group (**2ca**, IC_{50} = 212 nM) showed moderate activity. At R^1, only compounds with alkyl- and halide-substituted aryl sulfonyl ring were commercially available. 4-Methylphenyl and 2,5-dimethylphenyl reduced inhibition activity, whereas 3,4-dimethyl, 4-isopropyl, and 4-ethyl increased activity (compare **2bo** and **2cr**). Halide substitution also reduced activity (**2bi**). Having a two- or three-carbon hydrophobic group at the meta- and para-position of the aryl ring might increase activity because of tighter binding in the hydrophobic binding pocket of UT-B. Figure 2 summarizes the major findings of SAR analysis of commercially available analogues of **1**.

In vitro analysis of metabolic stability was done using LC/ESI-MS following compound incubation with hepatic microsomes in the presence of NADPH. Figure 1B shows the kinetics of microsomal degradation of selected compounds. Compound **1** showed rapid degradation with $t_{1/2} \approx 2.8$ min, with appearance of metabolic products at 16 AMU (+1 oxygen) and 32 (+2 oxygens) (Figure 1C). As observed by the relative growth of the peaks at $m/z = 472$ versus 488, the first oxidation

dx.doi.org/10.1021/jm300491y | J. Med. Chem. 2012, 55, 5942−5950

event appears to be more rapid than the second. We hypothesize that **1** undergoes rapid hydroxylation at either the benzylic[15] or thiophene-2-methylamine linking carbons, positions that are thought to stabilize radical intermediates (Figure 1D). As reported in Table S1, analogues with R^1 substituted with *p*-chlorophenyl showed greater in vitro metabolic stability (**2bf**–**2bj**), likely because of absence of the benzylic hydroxylation site and also because of occupation of the para-position, which is a known site of P450 metabolism.[16] Analogues with R^2 bearing the electron-rich benzylamine (**2ad**, **2aj**, **2bc**, **2bs**) also showed improved metabolic stability; however, these analogues had poor UT-B inhibition potency compared to **1**.

Synthesis of Triazolothienopyrimidine Analogues. SARs of commercial analogues of **1** indicated thiophene-2-methylamine as the best R^2 substituent for inhibition potency. The optimal R^1 substituent was not identified. We thus designed a library of focused analogues to fill in key elements of the SAR that were missing from the commercially available inhibitor set (Table 1), with the aim of maintaining or improving UT-B inhibition potency and improving metabolic stability. Most of the synthesized compounds were designed to maintain the R^2 substituent as thiophene-2-methylamine while investigating a small number of alkyl (**3a**, **3c**), alkoxy (**3d**, **3f**), halo (**3h**, **3i**), and heteroaryl (**3g**) substituents at R^1. A small number of inhibitors with variations of R^2 (substitutions for thiophene-2-methylamine) were also synthesized (**3b**, **3e**, and **3j**) to confirm the necessity of this heterocycle. One novel compound (**3k**), the 1,1-difluoroethyl analogue of **1**, was synthesized to be bioisosteric with ethyl but lacking the benzylic hydrogens that are likely involved in the rapid metabolism of **1**.

Our general synthetic approach toward the triazolothienopyrimidine scaffold is similar to that reported recently for synthesis of 5-HT_6 receptor antagonists.[17] The arylsulfonylacetonitrile building blocks were first synthesized (Scheme 1). Commercially available substituted arylthiols (**4a**–**4g**) were alkylated with bromoacetonitrile to generate the corresponding sulfides (**5a**–**5g**), which were then oxidized with mCPBA to give the desired arylsulfonylacetonitriles **6a**–**6g**. An additional variation of this building block (4-difluoroethylphenyl) was prepared by a multistep approach (Scheme 2) because the precursor benzenethiol was not commercially available. As such, 1-bromo-4-(1,1-difluoroethyl)benzene (**7**) was transformed under Pd-catalyzed conditions with the xanthphos ligand, analogous to the Buchwald–Hartwig reaction, to generate sulfide ester **8**. This was oxidized to sulfone **9**, converted to primary amide **10**, and dehydrated using phosphorus pentoxide to the desired 4-difluoroethylarylsulfoneacetonitrile (**6h**).

The second key synthetic precursor is a 3-azidothiophene ester (Scheme 3). 3-Bromothiophene-2-carboxaldehyde (**11**) was azidated by nucleophilic aromatic substitution to generate 3-azidothiophenecarboxaldehyde **12**. As reported previously,[14] aldehyde **12** was oxidized with the Lindgren reaction[18] to generate carboxylic acid **13**, which was alkylated with isobutyl bromide to 2-azidothiophene-1-isobutyl ester (**14**).

The attachment of the building blocks is shown in Scheme 4. The arylsulfonylacetonitriles **6a**–**6h** were reacted with base to form the nitrile enolates and coupled with the azidothiophene ester **14** followed by in situ lactamation to generate the core heterocycles (**15a**–**15h**). The use of isobutyl ester in **13** was to enhance stability compared to a methyl ester in order to prevent ester saponification during the cycloaddition–lactamation step, a side reaction that was observed in early optimization studies. Isobutyl ester was thought to afford stability during the base-promoted cycloaddition while being sufficiently reactive during the lactamation. The conversion of heterocycles **15a**–**15h** to the final library of amidine-containing compounds (**3a**–**3k**) was afforded with PyBOP during microwave irradiation. The use of PyBOP under microwave irradiation conditions was based on literature using the related

Table 1. UT-B Inhibition Activity[a] and Microsomal Stability[b] of Synthesized Compounds

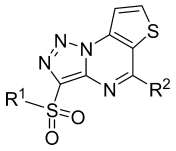

Cmpd	R^1	R^2	IC_{50} (nM)	% remaining[b]
1			11	<5
3a			153	<5
3b			16500	>99
3c			537	99
3d	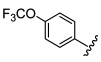		1110	95
3e		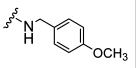	5290	7
3f	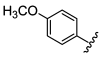		104	6
3g			196	<5
3h			468	27
3i			32	60
3j		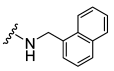	>2500	45
3k		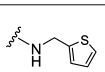	14	96

[a]Determined by mouse erythrocyte lysis assay (n = 3). IC_{50} determined by fit to a single-site saturation model. [b]Percentage of parent compound remaining after 30 min of incubation with rat liver microsomes.

dx.doi.org/10.1021/jm300491y | *J. Med. Chem.* 2012, 55, 5942–5950

Scheme 1. General Synthesis of Arylsulfonylacetonitrile Building Blocks[a]

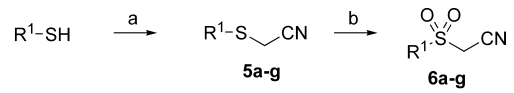

4a R^1= 4-isopropylphenyl
4b R^1= 4-trifluoromethylphenyl
4c R^1= 4-trifluoromethoxyphenyl
4d R^1= 4-methoxyphenyl
4e R^1= thiophene-2-yl
4f R^1= 4-fluorophenyl
4g R^1= 4-bromophenyl

[a]Reagents and conditions: (a) bromoacetonitrile, K_2CO_3, DMF, 2 h, rt; (b) mCPBA, CH_2Cl_2, 0 °C, 2 h.

Scheme 2. Synthesis of the Difluoroethylarylsulfonylacetonitrile Building Block[a]

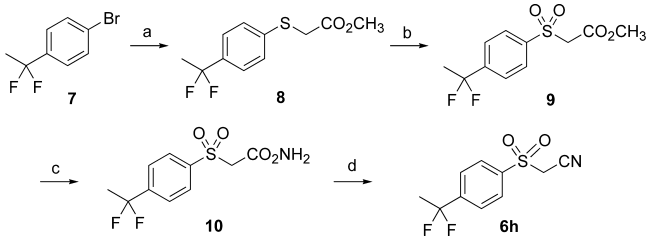

[a]Reagents and conditions: (a) methyl thioacetate, $Pd[PPh_3]_4$, xanthphos ligand, DIPEA, 1,4-dioxane, 135 °C, 16 h; (b) mCPBA, CH_2Cl_2, 0 °C, 2 h; (c) NH_3 in MeOH, 50 °C, 16 h; (d) phosphorus pentoxide, toluene, 75 °C, 1 h.

Scheme 3. Synthesis of the Azidothiophenyl Ester Building Block[a]

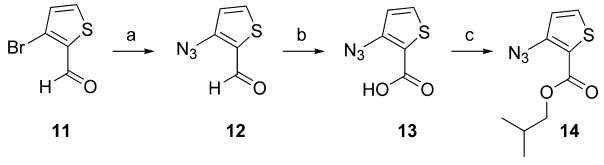

[a]Reagents and conditions: (a) NaN_3, DMSO, 65 °C, 48 h; (b) sodium chlorite, sulfamic acid, H_2O/acetone (1:1), 0 °C, 30 min; (c) isobutyl bromide, Cs_2CO_3, DMF, 80 °C, 6 h.

Scheme 4. Generation of Inhibitors via [2 + 3] Cycloaddition and Microwave-Assisted Dehydrative Amidine Coupling[a]

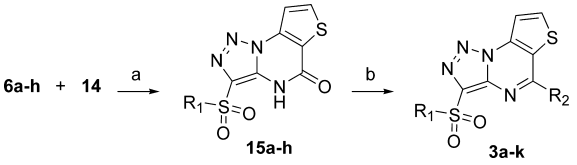

[a]Reagents and conditions: (a) NaOEt, EtOH, 30 min, rt; (b) amines, PyBOP, CH_3CN, microwave, 100 °C, 30 min.

reagent BOP without heating;[19,20] however, we found that the low-temperature conditions were not successful with triazolothienopyrimidines in the presence of BOP or PyBOP. With microwave assistance, PyBOP gave conversion to the desired amidine products, which was chosen over BOP because of its carcinogenic byproduct hexamethylphosphoramide (HMPA). $POCl_3$, which has been reported to activate the lactam in scaffold **15**,[17] gave low yields in our hands, possibly because of the relatively small reaction scale.

Potency and Metabolic Stability of Triazolothienopyrimidine Analogues. The IC_{50} and in vitro metabolic stability of synthesized analogues were determined (Table 1). In general, analogues lacking stabilized benzylic carbon for hydroxylation showed improved metabolic stability (**3c**, **3d**, **3i**). Fortunately, **3k** showed *both* excellent inhibition potency and metabolic stability and was further characterized. UT-B inhibition by **3k** was measured by stopped-flow light scattering, which provides a definitive measure of compound potency. The assay measures the kinetics of cell volume following rapid mixing of an erythrocyte suspension with a urea-containing solution. Figure 3A shows representative light scattering data for inhibition of UT-B urea transport in mouse erythrocytes. Each curve consists of a rapid upward phase, representing osmotic cell shrinkage, followed by a slower downward phase, representing urea (and water) influx. The kinetics of the downward phase was greatly slowed by **3k** in a concentration-dependent manner. Figure 3B summarizes concentration–inhibition data for mouse and human UT-B. Deduced IC_{50} values were 23 and 15 nM, respectively.

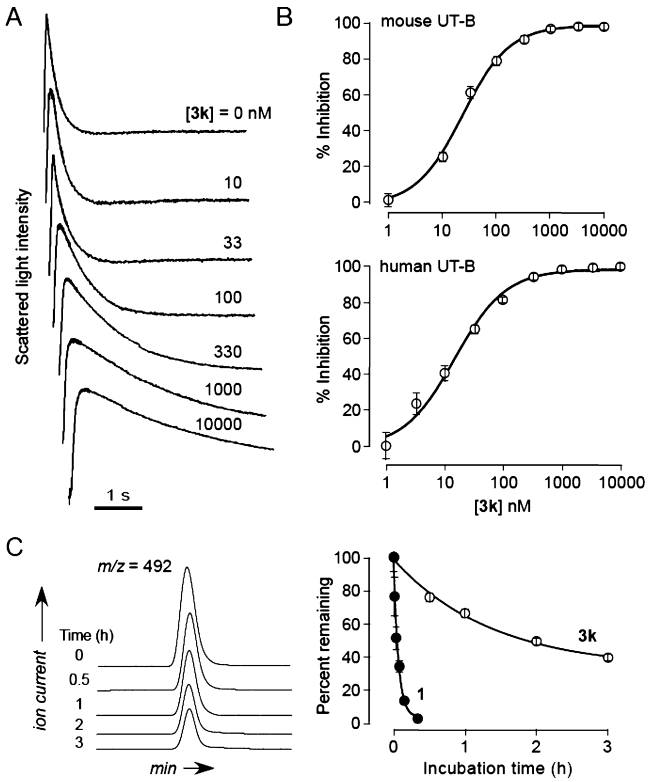

Figure 3. UT-B inhibition and in vitro metabolic stability of **3k**. (A) Stopped-flow light scattering measurement of urea permeability in mouse erythrocytes. Erythrocyte suspensions were mixed with an equal volume of urea-containing solution to give a 100 mM inwardly directed urea gradient. Inward urea flux is seen as decreasing scattered light intensity. Erythrocytes were incubated with indicated concentrations of **3k** for 10 min prior to measurements. (B) Concentration–inhibition data for mouse (top) and human (bottom) erythrocytes (SE, n = 3). Fitted IC_{50} values were 23 nM (mouse) and 15 nM (human). (C) In vitro metabolic stability in hepatic microsomes. (left) LC/MS showing kinetics of disappearance of **3k**. (right) Kinetics of **3k** disappearance, with data for **1** shown for comparison (SE, n = 3).

dx.doi.org/10.1021/jm300491y | J. Med. Chem. 2012, 55, 5942–5950

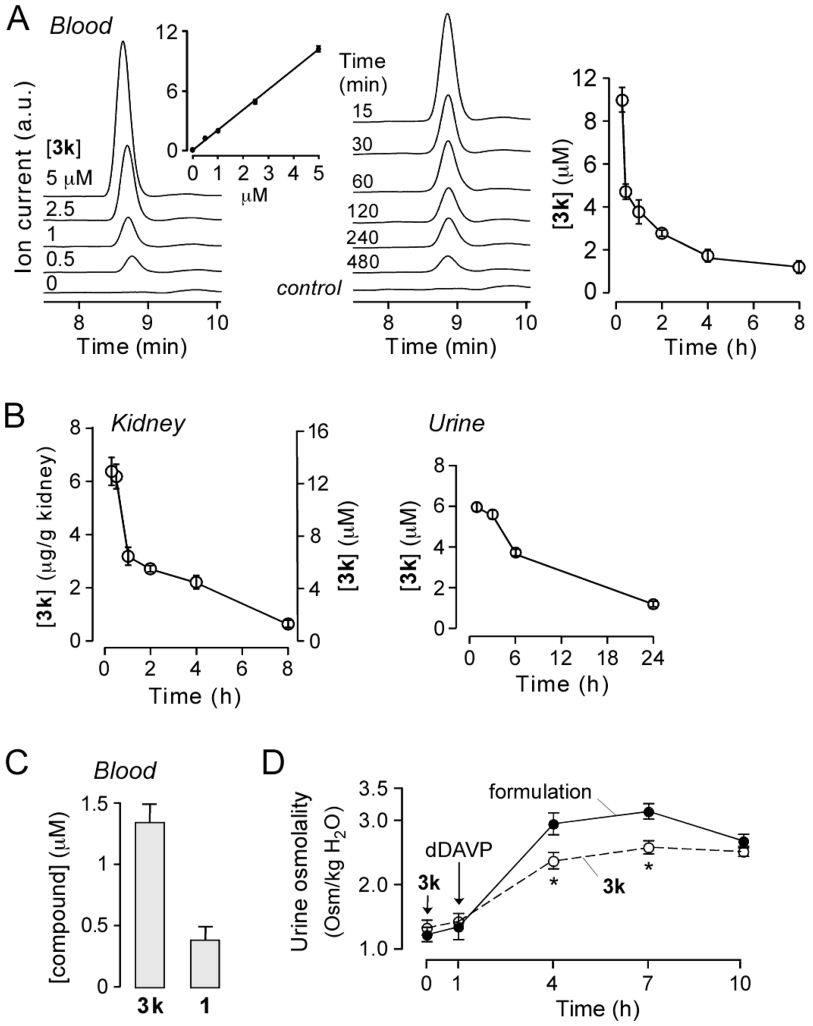

Figure 4. In vivo pharmacology and urearetic efficacy of **3k**. (A) LC/MS analysis of **3k** concentration in blood. Standards are shown at the left and inset. Also shown are original LC/MS traces and deduced **3k** concentrations in blood, following intraperitoneal bolus administration of 400 μg of **3k** (SE, 3 mice per group). (B) Concentrations of **3k** in kidney and urine for mice studied in (A). (C) Concentrations of **3k** and **1** in blood at 6 h after intraperitoneal administration of 200 μg of **3k** and 200 μg of **1** (SE, 3 mice). (D) Urine osmolality in mice after intraperitoneal administration of 400 μg of **3k** or formulation alone followed 1 h later by dDAVP (SE, 4 mice, (*) $P < 0.01$).

Figure 3C showed in vitro metabolic stability in hepatic microsomes. In parallel experiments, the $t_{1/2}$ for disappearance of **3k** was ~120 min, substantially slower than $t_{1/2}$ of ~2.8 min for disappearance of **1** shown for comparison. Thus, compared to **1**, compound **3k** is ~40-fold more stable in vitro while retaining comparable potency.

In Vivo Mouse Studies. The pharmacokinetics and renal accumulation of **3k** were measured in mice following intraperitoneal bolus administration of 400 μg of **3k** in a formulation chosen for efficient dissolution and absorption. Blood and kidney tissues were obtained at different times and **3k** was assayed by LC/MS after organic extraction, comparing with standards. Figure 4A show the LC/MS calibration for blood measurements (left), and the kinetics of **3k** concentration (right). Figure 4B shows the kinetics of **3k** concentration in kidney and urine. These data show high concentrations (>1 μM) of **3k** for many hours, well above its IC_{50} of ~25 nM for inhibition of UT-B urea transport. In a separate comparative study, mice received 200 μg of **3k** and **1** at the same time by intraperitoneal injection. At 6 h, the **3k** concentration was ~3-fold greater than that of **1** in blood (Figure 4C).

The urearetic activity of **3k** was assayed by measurement of urine osmolality in mice under maximal antidiuretic stimulation by the vasopressin analogue dDAVP. dDAVP was administrated 1 h after intraperitoneal injection of formulation, without or with **3k**. Figure 4D shows that dDAVP increased urine osmolality to >3 Osm/kg H_2O in control (formulation alone) mice, which was reduced by ~0.5 Osm/kg H_2O in mice receiving **3k**. This reduction in urine osmolality is similar to that produced by UT-B gene knockout.[6,14]

SUMMARY AND CONCLUSIONS

SAR analysis of triazolothienopyrimidine UT-B inhibitors, followed by rational synthesis of a focused library, identified **3k** as having excellent UT-B inhibition potency, with IC_{50} of 23 and 15 nM for mouse and human UT-B, respectively, and ~40-fold improved in vivo metabolic stability compared with **1**. The urearetic activity of **3k** was demonstrated in mice. In addition to prior data from knockout mice, the potential utility of UT-B inhibitors in humans is supported by the urinary concentrating defect in rare humans lacking UT-B.[21,22] UT inhibitors have a fundamentally different mechanism-of-action from conventional diuretics, which target kidney tubule salt transporters,

dx.doi.org/10.1021/jm300491y | J. Med. Chem. 2012, 55, 5942−5950

and so may act in synergy. Diuretics are used widely to increase renal salt and water excretion in fluid overload conditions such as congestive heart failure, cirrhosis, and nephrotic syndrome and when vasopressin levels are inappropriately high such as in the syndrome of inappropriate secretion of antidiuretic hormone (SIADH). By disrupting countercurrent mechanisms, UT inhibitors alone, or in combination with loop diuretics, may induce a diuresis in states of refractory edema where conventional diuretics are not effective.[23−25]

Several caveats are noted for further preclinical development of UT inhibitors. Demonstration of efficacy is needed in suitable animal disease models of fluid retention associated with heart or liver failure. Because UT-B is also expressed outside the kidney and mild extrarenal phenotypes have been reported in UT-B knockout mice,[26,27] thorough in vivo evaluation of inhibitor toxicity is necessary. The absence of extrarenal phenotypes in humans lacking UT-B is reassuring in this regard. Finally, we note that maximum urearetic action might be achieved by nonselective UT inhibitors that target UT-A isoforms as well.

METHODS

Chemistry. General Information. All solvents used in reactions were anhydrous and obtained from commercial sources unless otherwise specified. ^{1}H and ^{13}C NMR spectra were recorded on a Bruker DRX 300 MHz or Bruker Avance 500 MHz spectrometer. ^{1}H NMR chemical shifts are relative to TMS (δ = 0.00 ppm) or $CDCl_3$ (δ = 7.26 ppm). ^{13}C NMR chemical shifts are relative to $CDCl_3$ (δ = 77.23 ppm). Products were purified by flash column chromatography on silica gel (230−400 mesh). The eluent used for purification is reported in parentheses. Low-resolution LC/MS was performed using a Waters Micromass ZQ instrument or an Agilent-1100 HPLC instrument equipped with an Agilent 1956B mass spectrometer. High-resolution mass spectra were obtained by the University of Notre Dame Mass Spectrometry and Proteomics Facility (Notre Dame, IN) using ESI either by direct infusion on a Bruker micrOTOF-II or by LC elution via an ultrahigh pressure Dionex RSLC with C18 column coupled with a Bruker micrOTOF-Q II. Microwave-assisted organic synthesis was performed using a Biotage Isolera instrument. Thin layer chromatography (TLC) was done on aluminum sheet silica gel Merck 60F254. Commercial triazolothienopyrimidine analogues were purchased from ChemDiv (San Diego, CA). Some intermediates (**6a−6g**) are commercially available but were synthesized for the purpose of this study. Purity of all biologically evaluated compounds was >95% by RP-HPLC (254 nm) unless otherwise noted.

General Conditions for Conversion of Substituted Arylthiols (4) to Substituted Arylsulfonylacetonitriles (6). Bromoacetonitrile was dissolved in DMF (0.4 M), stirred in an ice bath, and then treated with substituted benzenethiol (**4**) (0.95 equiv) and K_2CO_3 (2 equiv), and the mixture was allowed to stir for 2 h at 0 °C. The reaction mixture was taken up into excess H_2O and extracted three times with Et_2O. The combined organic extracts were washed twice with water and brine, followed by concentration in vacuo to generate the intermediate aryl sulfide acetonitrile (**5**) in ∼90% yield. The sulfide was then dissolved in CH_2Cl_2 (0.4 M) and treated with mCPBA (77% peroxybenzoate, 2 equiv). The mixture was stirred at 0 °C under argon for 2 h to give complete conversion as monitored by TLC. The reaction mixture was quenched with excess sodium sulfite solution and extracted twice with CH_2Cl_2. The organic layer was washed with brine, dried over Na_2SO_4, and concentrated in vacuo to generate **6**.

[4-(1,1-Difluoroethyl)phenylsulfonyl]acetic Acid Methyl Ester (9). 1-Bromo-4-(1,1-difluoroethyl)benzene (**7**) (1000 mg, 4.52 mmol, 1.0 equiv) was treated with mercaptoacetic acid methyl ester (0.809 mL, 9.05 mmol, 2.0 equiv) in 1,4-dioxane (45 mL) and *N*-ethyldiisopropylamine (1.495 mL, 9.05 mmol, 2.0 equiv), tetrakis-(triphenylphosphine)palladium(0) (523 mg, 0.45 mmol, 0.1 equiv), 9,9-dimethyl-4,5-bis(diphenylphosphino)xanthene (451 mg, 0.91 mmol, 0.2 equiv). The mixture was heated at 135 °C under argon for 16 h. After cooling to room temperature, the mixture was filtered and the filtrate was concentrated under reduced pressure. The mixture was purified by flash column chromatography (hexanes/ethyl acetate = 6:1) to afford the sulfide (**8**) (yield 99%). The sulfide (1084 mg, 4.40 mmol) was dissolved in CH_2Cl_2 (44 mL) and oxidized by treatment with mCPBA (4341 mg, 17.61 mmol, 4.0 equiv) at 0 °C for 2 h. The reaction mixture was taken up in CH_2Cl_2 (150 mL) and was then washed with aqueous 5% Na_2SO_3 (3 × 50 mL). The organic layer was washed with brine, dried over Na_2SO_4, and concentrated in vacuo to yield **9** as a colorless oil. ^{1}H NMR ($CDCl_3$, 500 MHz): δ 1.97 (t, J = 15.0 Hz, 3H), 3.74 (s, 3H), 4.16 (s, 2H), 7.74 (d, J = 5.0 Hz, 2H), 8.04 (d, J = 10.0 Hz, 2H). ^{13}C NMR ($CDCl_3$, 125 MHz): δ 25.9 (t, J = 28.8 Hz), 53.4, 61.1, 126.0 (t, J = 6.3 Hz), 129.2, 134.6, 144.3, 162.9. ESI(+)-HRMS [M + Na]$^+$ calculated 301.0322, observed 301.0319 for $C_{11}H_{12}F_2O_4S$.

[4-(1,1-Difluoroethyl)benzenesulfonyl]acetonitrile (6h). The precursor methyl ester (**9**) (1232 mg, 4.43 mmol, 1.0 equiv) was added to a methanol solution of NH_3 (7 N) (15 mL, 132.8 mmol, 30 equiv) in the presence of catalytic NaCN (0.71 mg, 0.44 mmol, 0.1 equiv) in a sealed vial, and the mixture was heated at 50 °C for 16 h. The reaction mixture was extracted with CH_2Cl_2, washed with brine, and then concentrated in vacuo. The crude product was washed with ether and filtered to give the primary amide **10** which was used directly without purification or characterization. Amide **10** (500 mg, 1.90 mmol, 1.0 equiv) was dehydrated with phosphorus pentoxide (16175 mg, 56.98 mmol, 30 equiv) in toluene (95 mL) at 75 °C for 1 h. The reaction mixture was added to ice−water (300 mL) and then extracted with CH_2Cl_2 (200 mL). The aqueous layer was extracted with additional CH_2Cl_2 (3 × 50 mL), and the final organic layer was dried over Na_2SO_4. Purification by flash column chromatography (hexanes/ethyl acetate = 3:1) yielded the arylsulfonylacetonitrile **6h** as white needle-like crystals (146 mg, yield 31%). ^{1}H NMR ($CDCl_3$, 300 MHz): δ 1.97 (t, J = 18.0 Hz, 3H), 4.08 (s, 1H), 7.80 (d, J = 9.0 Hz, 2H), 8.12 (d, J = 6.0 Hz, 2H). ^{13}C NMR (acetone-d_6, 75 MHz): δ 24.6 (t, J = 29.3 Hz), 44.7, 111.2, 126.1 (t, J = 6.0 Hz), 129.2, 139.1, 144.2(t, J = 26.3 Hz). ESI(+)-HRMS [M + Na]$^+$ calculated 268.0220, observed 268.0190 for $C_{10}H_9F_2NO_2S$.

Isobutyl 3-Azidothiophene-2-carboxylate (14). Compound **13**[14] (5.8 g, 34.3 mmol) was treated with 1-bromo-2-methylpropane (4.47 mL, 1.2 equiv) and cesium carbonate (7.82 g, 0.7 equiv) in anhydrous DMF (0.1 M) and heated to 80 °C for 6 h under argon. The mixture was cooled, dissolved in H_2O (150 mL), and extracted with 1:1 diethyl ether/ethyl acetate (3 × 200 mL). The organic layer was washed with distilled H_2O (5 × 100 mL), dried over Na_2SO_4, and concentrated in vacuo to afford compound **14** as an amber oil (6.77 g, yield 77%). ^{1}H NMR ($CDCl_3$, 500 MHz): δ 1.00 (d, J = 10 Hz, 6H), 2.05 (m, 1H), 4.06 (d, J = 5 Hz, 2H), 6.91 (d, J = 5 Hz, 1H), 7.46 (d, J = 5 Hz, 1H). ^{13}C NMR ($CDCl_3$, 125 Hz): δ 19.8, 28.6, 71.8, 118.3, 122.8, 131.6, 142.8, 161.6. ESI(+)-LRMS [M + Na]$^+$ calculated 248.0, observed 247.8 for $C_9H_{11}N_3O_2S$.

General Conditions for Coupling of Substituted Arylsulfonylacetonitriles (6a−h) with Azidothiophene Ester (14) To Generate Cycloadducts (15a−h). Sodium ethoxide (2 mmol scale typically, 10 equiv based on starting material **14**) was dissolved in absolute ethanol (0.3 M), and then a substituted arylsulfonylacetonitrile (**6**) was added (1.5 equiv based on **14**). The mixture was stirred for 15 min at room temperature. Next, the 3-azidothiophene ester starting material (**14**) was added (1.0 equiv), and the mixture was stirred for 30 min at room temperature. TLC and HPLC analysis confirmed the consumption of starting material and formation of product. Solid $NaHCO_3$ (25 equiv) was added to neutralize the excess alkoxide base, and the reaction mixture was taken up into $CHCl_3$ and washed three times with aqueous 1 M HCl. The products were generally purified by crystallization with chloroform, with additional purification steps as specified.

3-(4-Isopropylbenzenesulfonyl)-4*H*-thieno[2,3-*e*][1,2,3]-triazolo[1,5-*a*]pyrimidin-5-one (15a). The crude product was purified by flash column chromatography using a gradient solvent system (CH_2Cl_2/Et_3N = 100:1 → CH_2Cl_2/CH_3OH/Et_3N = 100:2:1).

dx.doi.org/10.1021/jm300491y | J. Med. Chem. 2012, 55, 5942−5950

Yellow solid, yield 15%. ^{1}H NMR (DMSO-d_6, 300 MHz): δ 1.16 (d, J = 6 Hz, 6H), 2.93−3.07 (m, 1H), 7.25(d, J = 6 Hz, 1H), 7.42 (d, J = 9 Hz, 2H), 7.94 (d, J = 9 Hz, 2H), 8.05 (d, J = 6 Hz, 1H). ESI(+)-HRMS $[M + H]^+$ calculated 375.0585, observed 375.0574 for $C_{16}H_{14}N_4O_3S_2$. This compound is available commerically.

3-(4-Trifluoromethylbenzenesulfonyl)-4*H*-thieno[2,3-*e*][1,2,3]triazolo[1,5-*a*]pyrimidin-5-one (15b). The crude product was purified by flash column chromatography, using a gradient solvent system (CH_2Cl_2/Et_3N = 100:1 → CH_2Cl_2/CH_3OH/Et_3N = 100:2:1). The combined organics were taken up into chloroform, washed twice with aqueous 1 M HCl, dried over Na_2SO_4, and concentrated in vacuo to yield pure product. White solid, yield 5%. ^{1}H NMR ($CDCl_3$, 500 MHz): δ 7.85 (d, J = 5 Hz, 1H), 7.86 (d, J = 10 Hz, 2H), 8.06 (d, J = 5 Hz, 1H,), 8.25 (d, J = 10 Hz, 2H). ESI(+)-HRMS $[M + H]^+$ calculated 400.9990, observed 400.9982 for $C_{14}H_7F_3N_4O_3S_2$.

3-(4-Trifluoromethoxybenzenesulfonyl)-4*H*-thieno[2,3-*e*][1,2,3]triazolo[1,5-*a*]pyrimidin-5-one (15c). The crude product was purified by flash column chromatography (CH_2Cl_2/CH_3OH/Et_3N = 100:2:1). The combined organics were taken up into chloroform, washed twice with aqueous 1 M HCl, dried over Na_2SO_4, and concentrated in vacuo to yield pure product. White solid, yield 12%. ^{1}H NMR ($CDCl_3$, 500 MHz): δ 7.37 (d, J = 5 Hz, 1H), 7.73 (d, J = 5 Hz, 2H), 8.16 (d, J = 10 Hz, 1H), 8.30 (d, J = 10 Hz, 2H).

3-(4-Methoxybenzenesulfonyl)-4*H*-thieno[2,3-*e*][1,2,3]triazolo[1,5-*a*]pyrimidin-5-one (15d). The crude product was purified by flash column chromatography (CH_2Cl_2/CH_3OH/Et_3N = 100:2:1). The combined organics were taken up into chloroform, washed twice with aqueous 1 M HCl, dried over Na_2SO_4, and concentrated in vacuo to yield pure product. Yellow solid, yield 32%. ^{1}H NMR ($CDCl_3$, 300 MHz): δ 3.87 (s, 3H), 7.02 (d, J = 15 Hz, 2H), 7.84 (d, J = 10 Hz, 1H), 8.02 (d, J = 10 Hz, 1H,), 8.03 (d, J = 10 Hz, 2H). ESI(+)-HRMS $[M + H]^+$ calculated 363.0221, observed 363.0216 for $C_{14}H_{10}N_4O_4S_2$.

3-(Thiophene-2-sulfonyl)-4*H*-thieno[2,3-*e*][1,2,3]triazolo[1,5-*a*]pyrimidin-5-one (15e). Brown solid, yield 11%. ^{1}H NMR ($CDCl_3$, 300 MHz): δ 7.15−7.18 (m, 1H), 7.74 (d, J = 6 Hz, 1H), 7.86 (d, J = 6 Hz, 1H), 7.91 (d, J = 6 Hz, 1H), 8.04 (d, J = 6 Hz, 1H). ESI(+)-HRMS $[M + H]^+$ calculated 338.9680, observed 338.9677 for $C_{11}H_6N_4O_3S_3$.

3-(4-Fluorobenzenesulfonyl)-4*H*-thieno[2,3-*e*][1,2,3]triazolo[1,5-*a*]pyrimidin-5-one (15f). White solid, yield 43%. ^{1}H NMR ($CDCl_3$, 500 MHz): δ 7.85 (d, J = 5 Hz, 1H), 8.05 (d, J = 5 Hz, 1H), 8.13 (m, 2H). ESI(+)-HRMS $[M + Na]^+$ calculated 372.9842, observed 372.9832 for $C_{13}H_7FN_4O_3S_2$.

3-(4-Bromobenzenesulfonyl)-4*H*-thieno[2,3-*e*][1,2,3]triazolo[1,5-*a*]pyrimidin-5-one (15g). Yellow solid, yield 53%. ^{1}H NMR ($CDCl_3$, 500 MHz): δ 7.72 (d, J = 10 Hz, 2H), 7.85 (d, J = 5 Hz, 1H), 7.97 (d, J = 10 Hz, 2H), 8.05 (d, J = 5 Hz, 1H). ESI(+)-HRMS $[M + Na]^+$ calculated 432.9041, observed 432.9018 for $C_{13}H_7BrN_4O_3S_2$. This compound has been reported.[17]

3-(4-Difluoroethylbenzenesulfonyl)-4*H*-thieno[2,3-*e*][1,2,3]triazolo[1,5-*a*]pyrimidin-5-one (15h). White solid, yield 74%. ^{1}H NMR ($CDCl_3$, 300 MHz): δ 1.91 (t, J = 18.0 Hz, 3H), 7.70 (d, J = 9.0 Hz, 2H), 7.84 (d, J = 6.0 Hz, 1H), 8.04 (d, J = 3.0 Hz, 1H), 8.17 (d, J = 9.0 Hz, 2H). ESI(+)-HRMS $[M + H]^+$ calculated 397.0240, observed 397.0251 for $C_{15}H_{10}F_2N_4O_3S_2$.

General Conditions for Coupling of Heterocyclic Lactams (15a−h) with Primary Amines To Generate Triazolothienopyrimidines (3a−k). Heterocyclic lactam starting material (**15a−h**) (1 equiv) was dissolved in anhydrous CH_3CN (0.3 M) and treated with primary amine (3 equiv) and DBU (3 equiv) and PyBOP (3 equiv), and the mixture was irradiated by microwave at 100 °C for 30 min. The reaction was monitored by HPLC, showing consumption of starting material and formation of tentative product. The crude reaction mixture was treated with aqueous 1 M HCl (10 equiv) and stirred for 30 min at room temperature. Aqueous 1 M sodium carbonate solution was carefully added to adjust the pH to 9. The crude aqueous reaction mixture was extracted with ethyl acetate. The organic layer was washed three times with aqueous 1 M HCl, dried over Na_2SO_4, and concentrated in vacuo. The product was purified by precipitation and trituration with cold $CHCl_3$. Additional or alternative purification measures are provided as indicated.

[3-(4-Isopropylbenzenesulfonyl)thieno[2,3-*e*][1,2,3]triazolo[1,5-*a*]pyrimidin-5-yl]thiophen-2-ylmethylamine (3a). Crude product was purified by flash column chromatography using CH_2Cl_2/acetic acid (v/v = 100:1) to elute the starting materials first, then changing to CH_2Cl_2/CH_3OH/acetic acid (v/v/v = 100:2:1). Yellow solid, yield 21%. ^{1}H NMR (DMSO-d_6, 300 MHz): δ 1.17 (d, J = 9 Hz, 6H), 2.91−2.95 (m, 1H), 4.97 (d, J = 6 Hz, 2H), 7.03−7.04 (m, 1H), 7.23−7.24 (m, 1H), 7.39 (d, J = 9 Hz, 2H), 7.45−7.46 (m, 1H) 7.95−7.98 (m, 1H), 7.99−8.01 (m, 2H), 8.42 (d, J = 6 Hz, 1H), 9.48 (t, J = 3 Hz, 1H). ^{13}C NMR ($CDCl_3$, 125 Hz): δ 24.6, 34.6, 117.5, 126.5, 128.0, 128.3, 128.4, 138.0, 140.5, 155.5, 156.5. ESI(+)-HRMS $[M + H]^+$ calculated 470.0779, observed 470.0782 for $C_{21}H_{19}N_5O_2S_3$.

Furan-2-ylmethyl-[3-(4-isopropylbenzenesulfonyl)thieno[2,3-*e*][1,2,3]triazolo[1,5-*a*]pyrimidin-5-yl]amine (3b). Crude product was purified by flash column chromatography using CH_2Cl_2/acetic acid (v/v = 100:1) to elute the starting materials first, then changing to CH_2Cl_2/CH_3OH/acetic acid (v/v/v = 100:2:1). Yellow solid, yield 3%. ^{1}H NMR ($CDCl_3$, 500 MHz): δ 1.20 (d, J = 5 Hz, 6H), 2.92−2.94 (m, 1H), 4.20−4.23 (m, 2H), 7.05 (s, 1H), 7.17 (t, J = 5 Hz, 1H), 7.35 (d, J = 5 Hz, 2H), 7.53 (m, 1H), 8.14 (d, J = 5 Hz, 2H), 8.19 (d, J = 5 Hz, 1H), 8.36 (d, J = 5 Hz, 2H). This compound is commercially available and has also been reported.[17]

Thiophen-2-ylmethyl-[3-(4-trifluoromethylbenzenesulfonyl)thieno[2,3-*e*][1,2,3]triazolo[1,5-*a*]pyrimidin-5-yl]amine (3c). Crude product was purified by flash column chromatography using CH_2Cl_2/acetic acid (v/v = 100:1) to elute the starting materials first, then changing to CH_2Cl_2/CH_3OH/Et_3N (v/v/v = 100:1:1). White solid, yield 26%. ^{1}H NMR ($CDCl_3$, 300 MHz): δ 5.17 (d, J = 6 Hz, 2H), 7.04−7.05 (m, 1H), 7.51 (d, J = 6 Hz, 1H), 7.53 (d, J = 6 Hz, 1H), 7.68−7.71 (m, 2H), 7.93 (d, J = 6 Hz, 1H), 8.00 (d, J = 6 Hz, 1H), 8.33−8.35 (m, 2H). ESI(+)-HRMS $[M + H]^+$ calculated 400.9990, observed 400.9982 for $C_{14}H_7F_3N_4O_3S_2$.

Thiophen-2-ylmethyl-[3-(4-trifluoromethoxybenzenesulfonyl)thieno[2,3-*e*][1,2,3]triazolo[1,5-*a*]pyrimidin-5-yl]amine (3d). Additional purification involved prep-RP-HPLC. Yield 2%. ^{1}H NMR ($CDCl_3$, 500 MHz): δ 5.17 (d, J = 5 Hz, 2H), 5.80 (t, J = 5 Hz, 1H), 7.03−7.05 (m, 1H), 7.22 (d, J = 5 Hz, 1H), 7.25 (d, J = 10 Hz, 2H), 7.30 (d, J = 5 Hz, 1), 7.93 (d, J = 5 Hz, 1H), 8.00 (d, J = 5 Hz, 1H), 8.26 (d, J = 10 Hz, 2H). ESI(+)-HRMS $[M + H]^+$ calculated 512.0132, observed 512.0139 for $C_{19}H_{12}F_3N_5O_3S_3$.

[3-(4-Isopropylbenzenesulfonyl)thieno[2,3-*e*][1,2,3]triazolo[1,5-*a*]pyrimidin-5-yl]-(4-methoxybenzyl)amine (3e). The crude product was purified by flash column chromatography using CH_2Cl_2/acetic acid (v/v = 100:1) to elute the starting materials first and then changing to CH_2Cl_2/CH_3OH/acetic acid (v/v/v = 100:2:1). White solid, yield 20%. ^{1}H NMR ($CDCl_3$, 300 MHz): δ 1.21 (d, 6 H, J = 6 Hz), 2.89−2.93 (m, 1H), 4.92 (d, J = 6 Hz, 2H), 6.93 (d, J = 9 Hz, 2H), 7.17 (d, J = 3 Hz, 1H), 7.42 (d, J = 9 Hz, 2H), 7.89−7.91 (m, 2H), 7.97−7.98 (m, 1H), 8.12 (d, J = 9 Hz, 2H). LC/ESI-LRMS $[M + H]^+$ calculated 494.1 observed 494.0 for $C_{24}H_{23}N_5O_3S_2$.

[3-(4-Methoxybenzenesulfonyl)thieno[2,3-*e*][1,2,3]triazolo[1,5-*a*]pyrimidin-5-yl]thiophen-2-ylmethylamine (3f). The crude product was purified by flash column chromatography (CH_2Cl_2/CH_3OH/acetic acid = 120:1:1). Brown solid, yield 36%. ^{1}H NMR ($CDCl_3$, 500 MHz): δ 3.82 (s, 3H), 5.17 (d, J = 10 Hz, 2H), 6.90−6.93 (m, 2H), 7.04 (d, J = 5 Hz, 1H), 7.23 (d, J = 5 Hz, 1H), 7.30 (dd, J = 10 Hz, 5 Hz, 1H), 7.91 (d, J = 10 Hz, 1H), 8.00 (d, J = 10 Hz, 1H), 8.16 (d, J = 15 Hz, 2H). ^{13}C NMR ($CDCl_3$, 125 MHz): δ 41.0, 50.3, 114.7, 114.8, 118.1, 126.4, 127.9, 128.0, 134.0, 134.2, 139.2, 139.5, 140.2, 153.2, 164.1. ESI(+)-HRMS $[M + H]^+$ calculated 458.0415, observed 458.0421 for $C_{19}H_{15}N_5O_3S_3$.

[3-(Thiophene-2-sulfonyl)thieno[2,3-*e*][1,2,3]triazolo[1,5-*a*]-pyrimidin-5-yl]thiophen-2-ylmethylamine (3g). White solid, yield 10%. ^{1}H NMR (CD_3OD, 500 MHz): δ 5.09 (s, 2H), 6.98 (dd, J = 5 Hz, 1H), 7.08 (dd, J = 5 Hz, 1H), 7.23 (d, 1H), 7.29 (d, J = 5 Hz, 1H), 7.80 (dd, J = 10 Hz, 5 Hz, 1H), 7.82 (dd, J = 5 Hz, 1H), 7.96 (d, J = 5 Hz, 1H), 8.25 (d, J = 5 Hz, 1H).

[3-(4-Fluorobenzenesulfonyl)thieno[2,3-*e*][1,2,3]triazolo-[1,5-*a*]pyrimidin-5-yl]thiophen-2-ylmethylamine (3h). Yellow solid, yield 43%. ^{1}H NMR ($CDCl_3$, 500 MHz): δ 5.16 (d, J = 5 Hz, 2H), 5.74 (s, 1H), 7.04 (s, 1H), 7.11 (t, J = 5 Hz, 2H), 7.22(s, 1H), 7.31 (d, J = 5 Hz, 1H), 7.92 (d, J = 5 Hz, 1H), 8.00 (d, J = 5 Hz, 1H), 8.23(t, J = 5 Hz, 2H).

[3-(4-Bromobenzenesulfonyl)thieno[2,3-*e*][1,2,3]triazolo-[1,5-*a*]pyrimidin-5-yl]thiophen-2-ylmethylamine (3i). White solid, yield 35%. ^{1}H NMR ($CDCl_3$, 500 MHz): δ 5.16 (d, J = 5 Hz, 2H), 5.78 (t, J = 5 Hz, 1H), 7.04−7.06 (m, 1H), 7.32−7.33 (m, 1H), 7.33 (m, 1H), 7.58 (d, J = 10 Hz, 2H), 7.93 (d, J = 5 Hz, 1H), 8.00 (d, J = 5 Hz, 1H), 8.05 (d, J = 10 Hz, 2H). This compound is commercially available and has been reported.[17]

[3-(4-Isopropylbenzenesulfonyl)thieno[2,3-*e*][1,2,3]triazolo-[1,5-*a*]pyrimidin-5-yl]naphthalen-1-ylmethylamine (3j). Crude material was purified by flash column chromatography using CH_2Cl_2/acetic acid (v/v = 100:1) to elute the starting materials, then changed to CH_2Cl_2/CH_3OH/acetic acid (v/v/v = 100:2:1). White solid, yield 32%. ^{1}H NMR ($CDCl_3$, 500 MHz): δ 1.19 (d, J = 5 Hz, 6H,), 2.88 (m, 1H), 5.46 (d, J = 5 Hz, 2H), 5.61 (t, J = 5 Hz, 1H), 7.47−7.51 (m, 1H), 7.53 (d, J = 5 Hz, 2H), 7.55 (s, 1H), 7.56 (s, 1H), 7.62 (d, J = 5 Hz, 1H), 7.91 (d, J = 5 Hz, 1H), 7.95 (d, J = 5 Hz, 1H), 7.98 (d, J = 5 Hz, 1H), 8.10 (d, J = 5 Hz, 1H), 8.13 (d, J = 10 Hz, 2H). LC/ESI-LRMS $[M + H]^+$ calculated 514.1, observed 514.0 for $C_{27}H_{23}N_5O_2S_2$.

[3-[4-(1,1-Difluoroethyl)benzenesulfonyl]thieno[2,3-*e*]-[1,2,3]triazolo[1,5-*a*]pyrimidin-5-yl]thiophen-2-ylmethylamine (3k). After microwave irradiation, the reaction mixture was treated with aqueous 1 M HCl (10 equiv) and stirred for 10 min and then extracted three times with CH_2Cl_2. Combined organics were washed three times with aqueous 1 M HCl, dried over Na_2SO_4, and concentrated in vacuo. The product was precipitated by the addition of CH_3OH and isolated by vacuum filtration. The product **3k** was further purified by trituration with a small amount of $CHCl_3$ to give a white solid. Yield 15%. ^{1}H NMR (acetone-d_6, 300 MHz): δ 1.94 (s, J = 18.0 Hz, 3H), 5.15 (s, 2H), 7.01 (dd, J = 9.0, 3.0 Hz, 1H), 7.30−7.31 (m, 1H), 7.36−7.39 (m, 1H). 7.72 (d, J = 6.0 Hz, 2H), 7.97 (d, J = 6.0 Hz, 1H), 8.26 (d, J = 9.0 Hz, 2H), 8.34 (d, J = 6.0 Hz, 1H). ^{13}C NMR (acetone-d_6, 125 MHz): δ 25.0 (t, J = 28.8 Hz), 39.7, 114.5, 116.7, 125.3, 125.8 (t, J = 5.0 Hz), 127.0, 127.1, 127.0, 131.4, 135.6, 139.1, 141.0, 141.9, 142.6 (t, J = 27.5 Hz), 144.6, 153.7. ESI(+)-HRMS $[M + H]^+$ calculated 492.0356, observed 492.0423 for $C_{15}H_{10}F_2N_4O_3S_2$.

Blood Collection. Whole blood was collected from 8- to 12-week-old (25−35 g) wild-type mice in a CD1 genetic background by orbital puncture following subcutaneous injection of sodium heparin. Procedures were approved by the UCSF Committee on Animal Research. Human venous blood was collected into heparinized tubes, stored at 4 °C, and used within 48 h.

Erythrocyte Lysis Assay of UT-B Inhibition. Whole blood was diluted to a hematocrit of ∼1% in PBS containing 1.25 M acetamide and 5 mM glucose. Then 100 μL of the erythrocyte suspension was added to each well of a 96-well round-bottom microplate to which inhibitor was added from DMSO stock solution. After 10 min of incubation, 20 μL of the erythrocyte suspension was added rapidly to one well of a 96-well plate (Costar, Corning, NY) containing 180 μL of isosmolar buffer (PBS containing 1% DMSO). Erythrocyte lysis was quantified by absorbance at 710 nm, as described.[13] Percentage erythrocyte lysis was calculated using control values from the same plate as % lysis = $100 \times (A_{neg} - A_{test})/(A_{neg} - A_{pos})$, where A_{test} is the absorbance from a test well.

Stopped-Flow Measurement of Erythrocyte Urea Permeability. Measurements were done using a Hi-Tech Sf-51 instrument (Wiltshire, U.K.). Whole blood (mouse or human) was diluted in PBS (hematocrit of ∼0.5%), incubated with inhibitor for 5 min, and then subjected to a 100 mM inwardly directed urea gradient. The kinetics of increasing cell volume caused by urea influx was measured as the time-course of 90° scattered light intensity at 530 nm. Urea permeability and percentage inhibition were computed as described.[13]

In Vitro Metabolic Stability. Compounds (each 5 μM) were incubated for specified times at 37 °C with rat liver microsomes (1 mg protein/mL; Sigma-Aldrich, St. Louis, MO) in potassium phosphate buffer (100 mM) containing 1 mM NADPH. The mixture was then chilled on ice, and 0.5 mL of ice-cold ethyl acetate was added. Samples were centrifuged for 15 min at 3000 rpm. The supernatant was evaporated to dryness, and the residue was dissolved in 150 μL of mobile phase (acetonitrile:/water, 3:1, containing 0.1% formic acid) for LC/MS. Reverse-phase HPLC separations were carried out using a Waters C18 column (2.1 mm × 100 mm, 3.5 mm particle size) equipped with a solvent delivery system (Waters model 2690, Milford, MA). The solvent system consisted of a linear gradient from 5% to 95% acetonitrile run over 16 min (0.2 mL/min flow rate).

Mouse Studies. **3k** was formulated in 5% DMSO, 2.5% Tween-80, and 2.5% PEG400 in H_2O, as described.[14] Mice (age 8−10 weeks, 25−35 g) were administered 300 μL of formulation (without or with **3k**) by intraperitoneal injection. Urine, blood, and kidney samples were collected and processed as described.[14] dDAVP ([1-deamino-8-D-arginine]vasopressin, 1 μg/kg) was given 1 h after formulation. Urine osmolality was measured in water-diluted urine samples by freezing-point osmometry. Kidneys were homogenized in acetic acid (100 μL per 1 g of tissue) and ethyl acetate (10 mL per 1 g of tissue). The homogenate was centrifuged at 3000 rpm for 15 min. Calibration standards were prepared in kidney homogenates from untreated mice to which was added known amounts of **3k**. The ethyl acetate containing supernatant was dried under nitrogen and the residue dissolved in acetonitrile/H_2O (3:1) containing 0.1% formic acid. HPLC was done on a Xterra MS C18 column (2.1 mm × 100 mm, 3.5 μm particle size; Waters, Milford, MA) connected to a solvent delivery system (model 2690, Waters). The solvent system consisted of a linear gradient from 5% to 95% acetonitrile containing 0.1% formic acid over 16 min (0.2 mL/min flow). **3k** was detected by absorbance at 262 nm. Mass spectra were acquired on a mass spectrometer (Alliance HT 2790 + ZQ, Waters) using positive ion detection. For analysis of blood and urine, fluids were diluted with equal volumes of water and extracted with ethyl acetate.

■ ASSOCIATED CONTENT

Ⓢ Supporting Information

Table S1 summarizing potency and metabolic stability data for commercially available analogues of **1**. This material is available free of charge via the Internet at http://pubs.acs.org.

■ AUTHOR INFORMATION

Corresponding Author

*Phone: 415-338-6495. Fax: 415-405-0377. E-mail: marc@sfsu.edu.

Notes

The authors declare no competing financial interest.

■ ACKNOWLEDGMENTS

This work was supported by Grants DK35124, DK72517, DK86125, EB00415, HL73856, and EY13574 from the National Institutes of Health.

■ ABBREVIATIONS USED

UT, urea transporter; mCPBA, *m*-chloroperoxybenzoic acid; PyBOP, benzotriazol-1-yloxytripyrrolidinophosphonium hexafluorophosphate; BOP, benzotriazole-1-yloxy-tris-(dimethylamino)phosphonium hexafluorophosphate; HMPA, hexamethylphosphoramide; xanthphos, 4,5-bis-(diphenylphosphino)-9,9-dimethylxanthene; DMF, *N*,*N*-dimethylformamide; DMSO, dimethylsulfoxide

■ REFERENCES

(1) Bankir, L.; Trinh-Trang-Tan, M. M. Urea and the Kidney. In *The Kidney*. 6th ed.; Brenner, B. M., Ed.; WB Saunders: Philadelphia, PA, 2000; pp 637−679.

(2) Sands, J. M.; Layton, H. E. The physiology of urinary concentration: an update. *Semin. Nephrol.* **2009**, *29*, 178−195.
(3) Tsukaguchi, H.; Shayakul, C.; Berger, U. V.; Tokui, T.; Brown, D.; Hediger, M. A. Cloning and characterization of the urea transporter UT3: localization in rat kidney and testis. *J. Clin. Invest.* **1997**, *99*, 1506−1515.
(4) Sands, J. M. Renal urea transporters. *Curr. Opin. Nephrol. Hypertens.* **2004**, *13*, 525−532.
(5) Stewart, G. The emerging physiological roles of the SLC14A family of urea transporters. *Br. J. Pharmacol.* **2011**, *164*, 1476−5381.
(6) Yang, B; Verkman, A. S. Analysis of double knockout mice lacking aquaporin-1 and urea transporter UT-B. Evidence for UT-B-facilitated water transport in erythrocytes. *J. Biol. Chem.* **2002**, *277*, 36782−36786.
(7) Bankir, L.; Chen, K.; Yang, B. Lack of UT-B in vasa recta and red blood cells prevents urea-induced improvement of urinary concentrating ability. *Am. J. Physiol.: Renal Physiol.* **2004**, *286*, F144−F151.
(8) Fenton, R. A.; Chou, C. L.; Stewart, G. S.; Smith, C. P.; Knepper, M. A. Urinary concentrating defect in mice with selective deletion of phloretin-sensitive urea transporters in the renal collecting duct. *Proc. Natl. Acad. Sci. U.S.A.* **2004**, *101*, 7469−7474.
(9) Fenton, R. A.; Flynn, A.; Shodeinde, A.; Smith, C. P.; Schnermann, J.; Knepper, M. A. Renal phenotype of UT-A urea transporter knockout mice. *J. Am. Soc. Nephrol.* **2005**, *16*, 1583−1592.
(10) Fenton, R. A. Urea transporters and renal function: lessons from knockout mice. *Curr. Opin. Nephrol. Hypertens.* **2008**, *17*, 513−518.
(11) Uchida, S.; Sohara, E.; Rai, T.; Ikawa, M.; Okabe, M.; Sasaki, S. Impaired urea accumulation in the inner medulla of mice lacking the urea transporter UT-A2. *Mol. Cell. Biol.* **2005**, *25*, 7357−7363.
(12) Martial, S.; Neau, P.; Degeilh, F.; Lamotte, H.; Rousseau, B.; Ripoche, P. Urea derivatives as tools for studying the urea-facilitated transport system. *Pfluegers Arch.* **1993**, *423*, 51−58.
(13) Levin, M. H.; de la Fuente, R.; Verkman, A. S. Urearetics: a small molecule screen yields nanomolar potency inhibitors of urea transporter UT-B. *FASEB J.* **2007**, *21*, 551−563.
(14) Yao, C.; Anderson, M. O.; Zhang, J.; Yang, B.; Phuan, P.; Verkman, A. S. Triazolothienopyrimidine inhibitors of urea transporter UT-B reduce urine concentration. *J. Am. Soc. Nephrol.* [Online early access]. DOI: 10.1681/ASN.2011070751. Published Online: Apr 5, **2012**.
(15) Khojasteh-Bakht, S. C.; Rossulek, M. I.; Fouda, H. G.; Prakash, C. Identification of the human cytochrome P450s responsible for the in vitro metabolism of a leukotriene B4 receptor antagonist, CP-195,543. *Xenobiotica* **2003**, *33*, 1201−1210.
(16) Baldwin, S. J.; Clarke, S. E.; Chenery, R. J. Characterization of the cytochrome P450 enzymes involved in the in vitro metabolism of rosiglitazone. *Br. J. Clin. Pharmacol.* **1999**, *48*, 424−432.
(17) Ivachtchenko, A. V.; Golovina, E. S.; Kadieva, M. G.; Koryakova, A. G.; Kovalenko, S. M.; Mitkin, O. D.; Okun, I. M.; Ravnyeyko, I. M.; Tkachenko, S. E.; Zaremba, O. V. Synthesis and biological study of 3-(phenylsulfonyl)thieno[2,3-*e*][1,2,3]triazolo[1,5-*a*]pyrimidines as potent and selective serotonin 5-HT6 receptor antagonists. *Bioorg. Med. Chem.* **2010**, *18*, 5282−5290.
(18) Lindgren, B. O.; Nilsson, T.; Husebye, S.; Mikalsen, Ø.; Leander, K.; Swahn, C. G. Preparation of carboxylic acids from aldehydes (including hydroxylated benzaldehydes) by oxidation with chlorite. *Acta Chem. Scand.* **1973**, *27*, 888.
(19) Wan, Z. K.; Wacharasindhu, S.; Binnun, E.; Mansour, T. An efficent direct amination of cyclic amides and cyclic ureas. *Org. Lett.* **2006**, *8*, 2425−2428.
(20) Wan, Z. K.; Wacharasindhu, S.; Levins, C. G.; Lin, M.; Tabei, K.; Mansour, T. S. The scope and mechanism of phosphonium-mediated S_NAR reactions in heterocyclic amides and ureas. *J. Org. Chem.* **2007**, *72*, 10194−10210.
(21) Sands, J. M.; Gargus, J. J.; Frohlich, O.; Gunn, R. B.; Kokko, J. P. Urinary concentrating ability in patients with Jk(a-b-) blood type who lack carrier-mediated urea transport. *J. Am. Soc. Nephrol.* **1992**, *2*, 1689−1696.
(22) Lucien, N.; Sidoux-Walter, F.; Olives, B.; Moulds, J.; Le Pennec, P. Y.; Cartron, J. P.; Bailly, P. Characterization of the gene encoding the human Kidd blood group/urea transporter protein. Evidence for splice site mutations in Jknull individuals. *J. Biol. Chem.* **1998**, *273*, 12973−12980.
(23) Zhang, W.; Edwards, A. Theoretical effects of UTB urea transporters in the renal medullary microcirculation. *Am. J. Physiol.: Renal Physiol.* **2003**, *285*, F731−F747.
(24) Fenton, R. A. Essential role of vasopressin-regulated urea transport processes in the mammalian kidney. *Pfluegers Arch.* **2009**, *458*, 169−177.
(25) Smith, C. P. Mammalian urea transporters. *Exp. Physiol.* **2009**, *94*, 180−185.
(26) Guo, L.; Zhao, D.; Song, Y.; Meng, Y.; Zhao, H.; Zhao, X.; Yang, B. Reduced urea flux across the blood−testis barrier and early maturation in the male reproductive system in UT-B-null mice. *Am. J. Physiol.: Cell Physiol.* **2007**, *293*, C305−C312.
(27) Li, X.; Ran, J.; Zhou, H.; Lei, T.; Zhou, L.; Han, J.; Yang, B. Mice lacking urea transporter UT-B display depression-like behavior. *J. Mol. Neurosci.* **2012**, *46*, 362−372.